GMR
The Original

MULTITARGET NEUROPROTECTIVE POTENTIAL OF PHYTOCOMPOUNDS FROM GLYCYRRHIZA GLABRA: A NETWORK PHARMACOLOGY AND MOLECULAR DYNAMICS STUDY

Tharshanapriya K[1], Radha Palaniswamy[2]

[1]Research Scholar, Department of Biotechnology, Dr. N.G.P Arts and Science College, Coimbatore, Tamil Nadu, India, tharshana87biotech@gmail.com
[2]Associate Professor, Department of Biotechnology, Dr. N.G.P Arts and Science College, Coimbatore, Tamil Nadu, India.
radhapalaniswamy@drngpasc.ac.in

ABSTRACT
Neurodegenerative disorders are characterized by progressive neuronal loss associated with oxidative stress, neuroinflammation, apoptosis, and amyloid-beta accumulation. The present study aimed to investigate the neuroprotective potential of phytoconstituents identified from the ethanolic root extract of Glycyrrhiza glabra using an integrated GC–MS, network pharmacology, molecular docking, and molecular dynamics simulation approach. GC–MS analysis identified 43 phytocompounds, among which five biologically relevant compounds were selected for in silico analysis. Network pharmacology and protein–protein interaction analysis identified key hub genes including AKT1, EGFR, and BACE-1 associated with apoptosis, neuroinflammation, oxidative stress, and amyloid-beta response pathways. Functional enrichment analysis further confirmed the involvement of Alzheimer disease, neurotrophin signaling, and apoptotic pathways in neurodegenerative progression. Molecular docking studies revealed that 4H-pyran-4-one, 2,3-dihydro-3,5-dihydroxy-6-methyl- exhibited the strongest binding affinity against EGFR (−5.4 kcal/mol), AKT1 (−6.5 kcal/mol), and BACE-1 (−5.1 kcal/mol), supported by stable hydrogen bonding and hydrophobic interactions within the active binding pockets. Molecular dynamics simulations demonstrated stable protein–ligand complex formation throughout the 100 ns simulation period, with favorable RMSD, RMSF, SASA, radius of gyration, hydrogen bonding, and potential energy profiles. Collectively, the findings suggest that 4H-pyran-4-one, 2,3-dihydro-3,5-dihydroxy-6-methyl- possesses promising multitarget neuroprotective potential by modulating inflammatory, apoptotic, and amyloidogenic pathways implicated in neurodegenerative disorders. Further experimental validation is required to confirm its therapeutic applicability.

KEYWORDS: *Glycyrrhiza glabra*; Neurodegenerative disorders; GC–MS; Network pharmacology; Molecular docking; Molecular dynamics simulation; AKT1; EGFR; BACE-1; 4H-pyran-4-one, 2,3-dihydro-3,5-dihydroxy-6-methyl-; Neuroprotection.

1. INTRODUCTION

Neurodegenerative diseases encompassing Alzheimer's disease (AD), Parkinson's disease (PD), amyotrophic lateral sclerosis (ALS), and related disorders represent a growing global health crisis characterized by the progressive and irreversible deterioration of neuronal structure and function. The World Health Organization estimates that over 55 million people currently live with dementia worldwide, with AD accounting for 60–70% of all cases, and projections indicate this figure will triple to approximately 152 million by 2050 owing to rapidly ageing populations (WHO, 2023; Alzheimer's Association, 2023). Despite intensive pharmaceutical investment, approved disease-modifying therapies remain virtually absent, and available treatments continue to offer only symptomatic relief without halting or reversing underlying neuronal damage. This persistent and widening therapeutic gap has intensified the search for novel multi-target strategies capable of addressing the complex, interconnected molecular basis of neurodegeneration.

The pathophysiology of neurodegenerative diseases is fundamentally multi-factorial, driven by the convergence of chronic neuroinflammation, oxidative stress, mitochondrial dysfunction, aberrant protein aggregation, and dysregulated cell survival signalling. In AD specifically, abnormal cleavage of amyloid precursor protein (APP) by β-site APP cleaving enzyme 1 (BACE-1) generates neurotoxic amyloid-β (Aβ) peptides that accumulate into senile plaques, while hyperphosphorylated tau assembles into neurofibrillary tangles, together disrupting synaptic integrity and triggering neuronal apoptosis (Hardy & Selkoe, 2002; Selkoe & Hardy, 2016). Simultaneously, pro-inflammatory cytokines including interleukin-6 (IL-6) and tumor necrosis factor-α (TNF-α) sustain a chronic neuroinflammatory microenvironment that amplifies neuronal vulnerability (Heneka et al., 2015). The PI3K/AKT1 survival axis and epidermal growth factor receptor (EGFR)-mediated signaling further modulate the balance between neuronal survival and apoptosis, with their dysregulation directly exacerbating oxidative damage and neuronal loss (Lai et al., 2017). Therapeutic strategies capable of simultaneously targeting these interconnected nodes particularly BACE-1, AKT1, and EGFR hold considerable promise for meaningful disease modification.

In this context, medicinal plants have emerged as an invaluable resource for multi-target neuroprotective drug discovery, offering structurally diverse bioactive compounds with documented polypharmacological activities validated across centuries of traditional use (Balunas & Kinghorn, 2005; Newman & Cragg, 2020). *Glycyrrhiza glabra* Linn. (licorice) is

among the most historically significant and pharmacologically characterized medicinal plants, with documented use in Ayurvedic, Traditional Chinese, and Unani medicine systems for its anti-inflammatory, antioxidant, and neuroprotective properties (Fiore et al., 2005; Wang et al., 2015). Its rich phytochemical repertoire including glycyrrhizin, glabridin, liquiritigenin, isoliquiritigenin, and diverse flavonoid and chalcone derivatives has been linked to inhibition of neuroinflammatory cascades, reduction of Aβ production, attenuation of oxidative stress, and modulation of cholinergic neurotransmission in preclinical models (Simmler et al., 2013). Gas chromatography–mass spectrometry (GC–MS) profiling of the ethanolic extract of *G. glabra* root in the present study identified five pharmacologically relevant compounds 2',4'-dihydroxypropiophenone, 5-hydroxymethylfurfural (HMF), 4H-pyran-4-one (2,3-dihydro-3,5-dihydroxy-6-methyl-), theobromine, and 1,2-benzenediol selected on the basis of their antioxidant capacity, metal-chelating ability, neuromodulatory activity, and previously reported roles in mitigating oxidative and mitochondrial neuronal damage (Bak et al., 2016; Essa et al., 2012).

To systematically elucidate the molecular mechanisms underlying the neuroprotective activity of these compounds, the present study employed an integrated in silico framework combining network pharmacology, molecular docking, and molecular dynamics (MD) simulation. Network pharmacology, which models drug target disease interactions at a systems level through protein–protein interaction (PPI) network construction and pathway enrichment analysis, has become an indispensable tool for decoding the polypharmacological landscape of herbal preparations and identifying key therapeutic targets (Hopkins, 2008; Li & Zhang, 2013). Topological analysis of the constructed PPI network identified BACE-1, AKT1, and EGFR as the highest-priority hub targets implicated in neuroinflammation, apoptosis, and amyloidogenic processing, providing a rational basis for downstream structure-based investigations (Kibble et al., 2015). Molecular docking was subsequently performed to characterize the binding affinities and interaction geometries of the identified GC–MS compounds with these targets, followed by 100-nanosecond MD simulations to evaluate the thermodynamic stability and dynamic behavior of the resultant complexes through RMSD, RMSF, radius of gyration (Rg), solvent accessible surface area (SASA), potential energy, and hydrogen bond persistence analyses (Karplus & McCammon, 2002).

The integrated approach adopted here addresses the inherent limitations of single-target drug discovery paradigms by capturing the multi-pathway therapeutic potential of licorice bioactive compounds in a mechanistically coherent framework. The findings of this study are expected to provide molecular-level insights into the neuroprotective mechanisms of *G. glabra*-derived phytochemicals against key targets implicated in neurodegenerative pathology, and to establish a robust scientific rationale for future in vitro and in vivo experimental validation towards the development of plant-derived therapeutics for neurodegenerative disorders.

MATERIALS AND METHODS

Preparation of Plant Extract

Dried roots of *Glycyrrhiza glabra* Linn. were cleaned, shade-dried at room temperature, and ground into a fine powder using a mechanical grinder. The powdered plant material (100 g) was subjected to decoction with 500 mL of 95% ethanol kept in heating Mandle at 60°C. The extract was filtered through Whatman No. 1 filter paper then filtrates were concentrated using a rotary evaporator under reduced pressure at 40 °C, and the resultant crude extract was dried in a hot air oven at 40 °C to a constant weight. The percentage yield was calculated gravimetrically, and the dried extract was stored at −20 °C until further analysis (Azwanida, 2015).

GCMS Analysis

The ethanolic extract of dried roots of Glycyrrhiza glabra was analyzed by gas chromatography–mass spectrometry (GC–MS) at TÜV SÜD South Asia Pvt. Ltd. using a Thermo Scientific Trace GC Ultra coupled with an ISQ Single Quadrupole Mass Spectrometer equipped with a TG-5MS fused silica capillary column (15 m × 0.25 mm × 0.1 µm film thickness). Helium was used as the carrier gas at a constant flow rate of 1 mL/min. The injector and MS transfer line temperatures were maintained at 280°C, and electron ionization was carried out at 70 eV. The phytochemical constituents present in the extract were identified based on their retention times and mass spectral data by comparison with the NIST and Wiley library databases. The relative percentage composition of each compound was determined using peak area normalization (Soundararajan et al., 2021).

Network Pharmacology Analysis

A network pharmacology approach was employed to investigate the potential molecular mechanisms of the selected compound against neurodegenerative disorders. Genes associated with neurodegenerative diseases were retrieved from the GeneCards database using keywords such as "neurodegenerative disease," "Alzheimer's disease," and "Parkinson's disease." The common targets shared between compound-related targets and disease-associated genes were identified through Venn analysis and considered as potential therapeutic targets. These overlapping genes were subsequently imported into the STRING database to construct a protein–protein interaction (PPI) network, with the organism limited to Homo sapiens and an appropriate confidence score threshold applied. The PPI network was visualized and analyzed using Cytoscape, and hub genes were identified based on topological parameters including degree, betweenness centrality, and closeness centrality. Furthermore, functional enrichment analyses, including Gene Ontology (GO) and Kyoto Encyclopedia of Genes and Genomes (KEGG) pathway analyses, were performed using the GSEApy package. Significantly enriched biological processes and signaling pathways were selected based on adjusted p-values and visualized to elucidate the possible therapeutic mechanisms of the selected compound against neurodegenerative disorders (Wang et al., 2024; Dio Syahputra et al., 2024).

Ligand Selection and Preparation

The bioactive compounds identified from the GC–MS analysis of the ethanolic root extract of Glycyrrhiza glabra were selected as ligands for molecular docking studies. The selected compounds included 2',4'-Dihydroxypropiophenone, 5-Hydroxymethylfurfural (HMF), 4H-Pyran-4-one, 2,3-dihydro-3,5-dihydroxy-6-methyl-, Theobromine, and 1,2-

Benzenediol. The three-dimensional structures of the selected ligands were retrieved from the PubChem database in SDF format and converted into PDB format using Open Babel. The ligand structures were further energy minimized, hydrogen atoms were added, and appropriate bond orders were assigned prior to docking analysis. Finally, the prepared ligands were saved in PDBQT format for subsequent molecular docking studies (Sinha et al., 2020).

Receptor Selection and Preparation

The crystal structures of the selected target proteins, including Epidermal Growth Factor Receptor (PDB ID: 1IVO), AKT Serine/Threonine Kinase 1 (PDB ID: 3O96), and Beta-Secretase 1 (PDB ID: 6EQM), were retrieved from the RCSB Protein Data Bank in PDB format. The receptor structures were prepared by removing co-crystallized ligands, water molecules, and other heteroatoms, followed by the addition of polar hydrogen atoms and Kollman charges. The prepared protein structures were subsequently converted into PDBQT format and used as receptors for molecular docking studies (Kura et al., 2024).

Molecular Docking

Molecular docking studies were performed using the AutoDock Vina algorithm implemented in PyRx 0.8 with a maximized grid spacing strategy. The prepared receptor proteins and energy-minimized ligands were imported into the Vina Wizard, and the grid box dimensions were configured to completely cover the active binding sites of the target proteins. Docking simulations were conducted with the exhaustiveness parameter set to 8 and the number of generated binding poses limited to 9 for accurate prediction of ligand–protein interactions. The best docking conformations obtained were subsequently visualized and analysed using BIOVIA Discovery Studio Visualizer to examine the molecular interactions and binding affinities between the selected ligands and receptor proteins (Selvaraj et al., 2024; Kura et al., 2024).

Molecular Dynamic Simulation

Molecular dynamics (MD) simulations were performed using GROMACS 2024.3 with the CHARMM36 force field applied for proteins and GAFF2 parameters assigned for the ligands (Lindorff-Larsen et al., 2010). The protein–ligand complexes were positioned in a cubic simulation box under periodic boundary conditions, solvated with explicit water molecules, and neutralized by adding counter ions at physiological ionic strength. Long-range electrostatic interactions were calculated using the particle mesh Ewald (PME) method, while van der Waals interactions were treated using a force-switch cutoff scheme. Hydrogen-containing bonds were constrained using the LINCS algorithm, permitting the use of a 2 fs integration time step. Each system initially underwent energy minimization using the steepest descent algorithm, followed by equilibration under the NVT ensemble for 1 ns and the NPT ensemble for 2 ns using a velocity-rescale thermostat and Parrinello–Rahman barostat. Subsequently, a 100 ns production simulation was carried out under NPT conditions. The generated trajectories were further analysed using standard GROMACS utilities to determine root mean square deviation (RMSD), root mean square fluctuation (RMSF), radius of gyration (Rg), hydrogen bond interactions, solvent-accessible surface area (SASA), and centre-of-mass distances to evaluate the structural stability and interaction behaviour of the complexes (Archana et al., 2023).

RESULT

GCMS analysis

GC-MS analysis of the ethanolic extract of dried roots of *Glycyrrhiza glabra* Linn led to the identification of 43 (Table1; Figure1) volatile and semi-volatile constituents across a retention time range of 4.19–20.91 min, with compound identification achieved through NIST11.L spectral library matching. Among the identified phytoconstituents, five biologically relevant compounds were selected for further in silico investigation based on their structural diversity, abundance, and pharmacological significance in the context of neurodegeneration. 2′,4′-Dihydroxypropiophenone (RT 9.46 min; Area% 0.95%; match score 65.6), a hydroxylated propiophenone belonging to the chalcone-related phenolic class, was identified for its potent antioxidant capacity and established enzyme inhibitory properties relevant to cholinergic modulation. 5-Hydroxymethylfurfural (HMF) (RT 7.34 min; Area% 3.59%; match score 96.5), detected with the highest spectral confidence in the dataset, was selected on account of its significant chromatographic abundance and documented neuroprotective activity through attenuation of oxidative and mitochondrial stress in neuronal cells. 4H-Pyran-4-one, 2,3-dihydro-3,5-dihydroxy-6-methyl- (DDMP; RT 6.56 min; Area% 2.64%; match score 90.0), a Maillard-derived heterocyclic compound with a β-diketone motif, was included owing to its metal-chelating capacity, which confers potential inhibitory activity against metal-induced amyloid aggregation and associated oxidative cascades implicated in Alzheimer's disease pathology. 1,2-Benzenediol (catechol; RT 6.99 min; Area% 0.54%), a catecholic phenol with known antioxidant, anti-inflammatory, and enzyme-modulating properties, was incorporated for its structural relevance to endogenous catecholamine metabolism and its capacity to mitigate oxidative neuronal damage. Finally, theobromine (RT 12.84 min; Area% 3.53%; match score 92.0), a dimethylxanthine alkaloid detected at relatively high abundance, was selected for its established neuromodulatory activity mediated through adenosine receptor antagonism and its influence on downstream neuronal signalling pathways. Collectively, these five structurally diverse phytoconstituents, spanning phenolics, furan derivatives, pyranones, and alkaloids, represent multi-target bioactive candidates capable of addressing the oxidative, cholinergic, metal-dysregulation, and neuromodulatory axes implicated in neurodegenerative disorders, and were accordingly advanced for network pharmacology and molecular docking analyses.

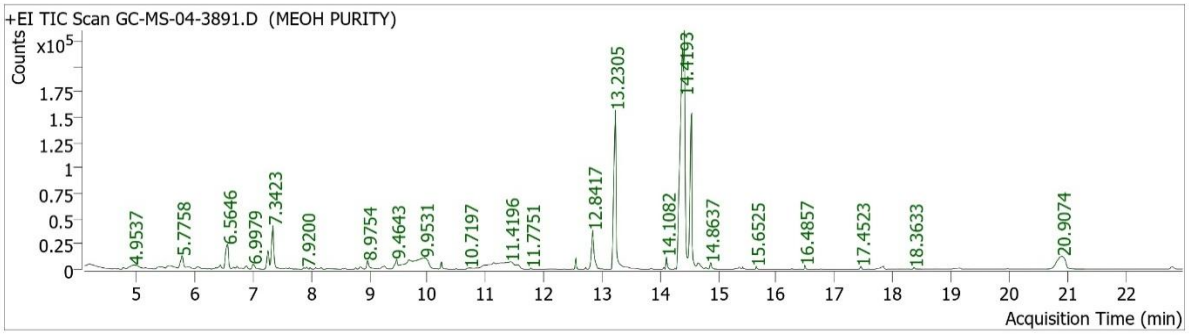

Figure 1: GCMS Chromatogram

Table 1. GC-MS analysis of ethanolic extract of Glycyrrhiza glabra Linn (dried roots)

S. No.	RT (min)	Compound Name	Peak Area	Area%-T
1	4.1871	2-Cyclopenten-1-one, 2-hydroxy-	6,957	0.21
2	4.7648	2,4-Dihydroxy-2,5-dimethyl-3(2H)-furan-3-one	4,659	0.14
3	4.9537	Oxalic acid, allyl ethyl ester	46,087	1.37
4	5.4314	7-Tridecylamine	20,660	0.61
5	5.5647	2,4,5-Trihydroxypyrimidine	32,522	0.97
6	5.7758	D-Alanine, N-propargyloxycarbonyl-, propargyl ester	50,024	1.49
7	6.0536	2-Propen-1-ol	12,017	0.36
8	6.2424	Propanoic acid, 2-acetylhydrazono-	1,814	0.05
9	6.4313	Ethanamine, N-ethyl-N-nitroso-	18,722	0.56
10	6.5646	4H-Pyran-4-one, 2,3-dihydro-3,5-dihydroxy-6-methyl-	89,046	2.64
11	6.6535	Propanedioic acid, oxo-, diethyl ester	6,217	0.18
12	6.7201	1-Aminocyclopentanecarboxylic acid, N-methoxycarbonyl-, heptyl ester	7,638	0.23
13	6.8868	Azetidine, 1,1'-methylenebis[2-methyl-	10,531	0.31
14	6.9979	1,2-Benzenediol, o-valeryl-	18,092	0.54
15	7.2534	3-Thiopheneethanol	45,818	1.36
16	7.3423	5-Hydroxymethylfurfural	1,21,000	3.59
17	7.6200	2,5-Furandicarboxaldehyde	4,440	0.13
18	7.9200	1-(Methylthio)-3-pentanone	6,883	0.20
19	7.9756	2-Furanbutanoic acid, γ-oxo-	2,637	0.08
20	8.1644	4-Acetoxy-3-methoxystyrene	3,944	0.12
21	8.2866	2-Butanol, 3-(1,3,3-trimethylbutoxy)-	5,064	0.15
22	8.7644	1-Tetrazol-2-ylethanone	2,403	0.07
23	8.8421	4-Octanol, 2,7-dimethyl-	7,356	0.22
24	8.9754	Benzene, 1-chloro-2-methoxy-	27,837	0.83
25	9.4643	2',4'-Dihydroxypropiophenone	32,085	0.95
26	9.6754	Vinyl caprylate	95,263	2.83
27	9.9531	Sucrose	1,64,646	4.89
28	10.2420	Dodecanoic acid	14,561	0.43
29	10.4864	Methyl(3,3-difluoro-2-propenyl)difluorosilane	802	0.02
30	10.7197	Uracil	3,992	0.12
31	11.1419	1,3,5-Trimethyl-1H-pyrazol-4-amine	2,819	0.08
32	11.4196	7-Oxo-1,3,5-cycloheptatriene-1-carbonitrile	16,755	0.50
33	11.5529	Methane, dipropoxy-	7,179	0.21
34	11.7751	O-Methyl-DL-serine, N-dimethylaminomethylene-, butyl ester	1,255	0.04
35	12.5528	Caffeine	15,555	0.46
36	12.8417	Theobromine	1,18,990	3.53
37	13.2305	n-Hexadecanoic acid	4,72,756	14.03
38	14.1082	Dodecanoic acid, 2,3-dihydroxypropyl ester	18,850	0.56
39	14.4193	6-Octadecenoic acid	12,71,098	37.73
40	14.5415	Octadecanoic acid	3,84,332	11.41
41	14.6526	Bicyclo[4.1.0]heptane, 7-pentyl-	29,496	0.88
42	14.7859	3-Hexyne, 2-methyl-	3,955	0.12
43	14.8637	Bicyclo[4.1.0]heptane, 7-pentyl- (2nd peak)	14,337	0.43
44	15.6525	Eicosanoic acid	3,077	0.09
45	16.4857	Hexadecanoic acid, 2-hydroxy-1-(hydroxymethyl)ethyl ester	5,028	0.15

46	17.4523	4-Fluorobenzylamine, N,N-dinonyl-	4,821	0.14
47	18.3633	Barbituric acid	3,236	0.10
48	20.9074	Dodecanoic acid, 1-(hydroxymethyl)-1,2-ethanediyl ester	1,31,365	3.90

Protein–Protein Interaction Network Analysis and Hub Gene Identification

Topological analysis of the constructed protein–protein interaction (PPI) network identified ten hub genes — BACE-1, IL-6, TNF, AKT1, TP53, BCL2, EGFR, CTNNB1, MYC, and ALB (Fig2A) based on their degree centrality, betweenness, and closeness scores, indicating a highly interconnected regulatory architecture underlying neurodegenerative pathogenesis. Among these, the pro-inflammatory mediators BACE-1, IL-6, and TNF constituted a central signaling axis, underscoring the pivotal role of chronic neuroinflammation in disease progression. Apoptosis-regulatory proteins TP53 and BCL2 were co-identified, suggesting a disrupted equilibrium between neuronal survival and programmed cell death. The cell survival and proliferation kinase AKT1, together with the receptor tyrosine kinase EGFR, highlighted the involvement of growth factor-mediated signaling cascades, while CTNNB1 implicated Wnt pathway dysregulation, a mechanism critical for synaptic integrity and neuronal maintenance. MYC contributed to transcriptional dysregulation, further reflecting the complexity of gene regulatory networks in neurodegeneration. Although ALB emerged as a topological hub owing to its high network connectivity, it was considered a non-specific interaction partner rather than a direct mechanistic contributor and was excluded from downstream analyses. Based on collective topological significance and mechanistic relevance, AKT1, EGFR, and BACE-1 were prioritized as representative targets for subsequent molecular docking and simulation studies, collectively capturing the interplay among survival signaling, receptor-mediated pathways, and neuroinflammatory responses.

Gene Ontology and Pathway Enrichment Analysis

Functional enrichment analysis demonstrated that the identified hub genes are significantly associated with key biological processes and molecular pathways implicated in neurodegeneration. Among the most enriched Gene Ontology (GO) (Fig2B) terms, cysteine-type endopeptidase activity involved in the execution phase of apoptosis was prominently represented, indicating a strong contribution of caspase-mediated mechanisms to neuronal cell death. Pathways directly associated with Alzheimer disease and cellular response to amyloid-beta confirmed the disease-specific relevance of the identified gene set. Neuroinflammatory pathway enrichment, encompassing both regulation and positive regulation of neuroinflammatory response, reinforced the central mechanistic contribution of cytokine-driven inflammation, particularly via BACE-1, IL-6, and TNF. The enrichment of neurotrophin signaling and serotonergic synapse pathways further indicated disruption of neuronal survival, synaptic transmission, and plasticity. Additionally, the identification of axon guidance and xenobiotic transport across the blood–brain barrier pathways suggested impairment of neuronal connectivity and altered molecular trafficking within the brain microenvironment. Collectively, these findings demonstrate that the selected hub genes are functionally enriched across interconnected processes of apoptosis, inflammation, and synaptic dysfunction, providing robust biological justification for the selection of AKT1, EGFR, and BACE-1 as therapeutic targets.

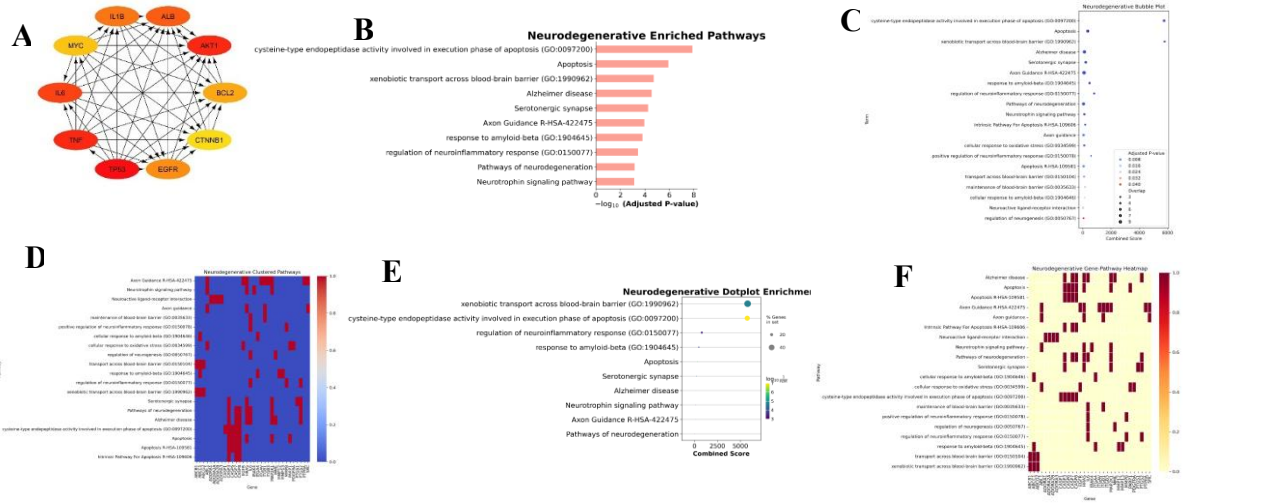

Figure 2: Networking Pharmacology. A) Cytoscape, B)Bar Plot, C) Bubble Plot, D) Clustered Pathway, E) Dot Plot, F) Heat Map

Bubble Plot and Dot Plot Visualization of Enriched Pathways

Bubble plot and dot plot analyses were employed to visually quantify the functional enrichment significance of the identified gene set across neurodegenerative pathways. The highest combined enrichment scores were observed for cysteine-type endopeptidase activity involved in the execution phase of apoptosis and intrinsic apoptotic signaling pathways, confirming the centrality of caspase-mediated neuronal death (Fig2C). High combined scores for apoptosis, Alzheimer disease, and response to amyloid-beta collectively indicated strong involvement in classical neurodegenerative pathology. Dot plot (Fig2D) analysis further corroborated these findings, with xenobiotic transport across the blood–brain barrier and apoptosis execution pathways exhibiting the highest gene ratio and statistical significance. Pathways including regulation of neuroinflammatory response, response to amyloid-beta, neurotrophin signaling, serotonergic synapse, and axon guidance were consistently enriched across both visualizations, reflecting coordinated disruptions in neuronal

communication, synaptic plasticity, and barrier integrity. The enrichment of cellular response to oxidative stress in both plots further affirmed the role of reactive oxygen species-mediated damage in neurodegenerative progression. Taken together, the bubble and dot plot analyses demonstrate multidimensional functional enrichment of the identified targets, providing strong quantitative support for the selection of AKT1, EGFR, and BACE-1 for downstream therapeutic investigation.

Pathway–Gene Heatmap Analysis

Clustered pathway–gene heatmap (Fig2F) analysis revealed distinct functional modules among the identified genes across neurodegenerative pathways, demonstrating coordinated and non-random biological organization. A prominent apoptosis-associated cluster was observed, encompassing cysteine-type endopeptidase activity, intrinsic apoptotic signaling, and general apoptosis pathways, reflecting strong caspase-associated gene involvement in neuronal cell death. A second major cluster corresponded to Alzheimer disease and response to amyloid-beta, confirming disease-specific pathway relevance of the identified gene set. A distinct inflammatory cluster, comprising regulation and positive regulation of neuroinflammatory response, highlighted the contribution of cytokine-mediated mechanisms. Genes involved in axon guidance, neurotrophin signaling, and serotonergic synapse pathways were grouped within a separate functional module, suggesting coordinated disruption of neuronal communication, synaptic plasticity, and neurodevelopmental processes. Additional clustering of genes participating in oxidative stress response and blood–brain barrier transport indicated alterations in cellular homeostasis and impaired molecular trafficking within the brain microenvironment. The gene–pathway distribution further confirmed that individual genes participate in multiple overlapping biological processes, reinforcing the concept that neurodegeneration is governed by the coordinated interplay of apoptosis, inflammation, oxidative stress, and synaptic dysfunction. Collectively, the heatmap analyses provide strong systems-level evidence supporting the selection of AKT1, EGFR, and BACE-1 as key mechanistic targets for molecular docking and therapeutic investigation in neurodegenerative disorders.

Molecular Docking

Human EGFR

The molecular docking analysis of the selected phytocompounds against Epidermal Growth Factor Receptor revealed varying binding affinities across the nine generated docking conformations (Table2). Among all the tested compounds, 4H-pyran-4-one, 2,3-dihydro-3,5-dihydroxy-6-methyl- exhibited the strongest binding affinity with a docking score of −5.4 kcal/mol, indicating a favorable interaction with the active binding pocket of EGFR. The ligand formed a conventional hydrogen bond with the SER291 residue, which plays an important role in stabilizing the protein–ligand complex. In addition, surrounding amino acid residues including TYR292, GLU293, GLY288, CYS287, CYS309, VAL312, SER340, SER342, THR378, and ALA286 contributed through van der Waals interactions, further enhancing the stability of the complex (Fig3A). Other identified compounds such as 2',4'-Dihydroxypropiophenone, Theobromine, 5-Hydroxymethylfurfural, and 1,2-Benzenediol showed comparatively lower binding affinities ranging from −5.3 to −4.2 kcal/mol. The presence of hydrogen bonding together with multiple non-bonded interactions suggests that 4H-pyran-4-one, 2,3-dihydro-3,5-dihydroxy-6-methyl- may serve as a promising bioactive compound targeting EGFR-associated neurodegenerative pathways.

Ligand	Target Protein	Binding Affinity (kcal/mol)
4H-Pyran-4-one, 2,3-dihydro-3,5-dihydroxy-6-methyl-	EGFR (1IVO)	-5.4
5-Hydroxymethylfurfural (HMF)	EGFR (1IVO)	-5.1
2',4'-Dihydroxypropiophenone	EGFR (1IVO)	-5.0
Theobromine	EGFR (1IVO)	-5.3
1,2-Benzenediol	EGFR (1IVO)	-5.1
4H-Pyran-4-one, 2,3-dihydro-3,5-dihydroxy-6-methyl-	AKT1 (3O96)	-6.2
5-Hydroxymethylfurfural (HMF)	AKT1 (3O96)	-5.2
2',4'-Dihydroxypropiophenone	AKT1 (3O96)	-4.9
Theobromine	AKT1 (3O96)	-5.6
1,2-Benzenediol	AKT1 (3O96)	-6.5
4H-Pyran-4-one, 2,3-dihydro-3,5-dihydroxy-6-methyl-	BACE-1 (6EQM)	-4.5
5-Hydroxymethylfurfural (HMF)	BACE-1 (6EQM)	-4.3
2',4'-Dihydroxypropiophenone	BACE-1 (6EQM)	-5.0
Theobromine	BACE-1 (6EQM)	-4.9
1,2-Benzenediol	BACE-1 (6EQM)	-5.1

Table 2: Molecular docking binding affinities of selected phytocompounds against EGFR, AKT1, and BACE

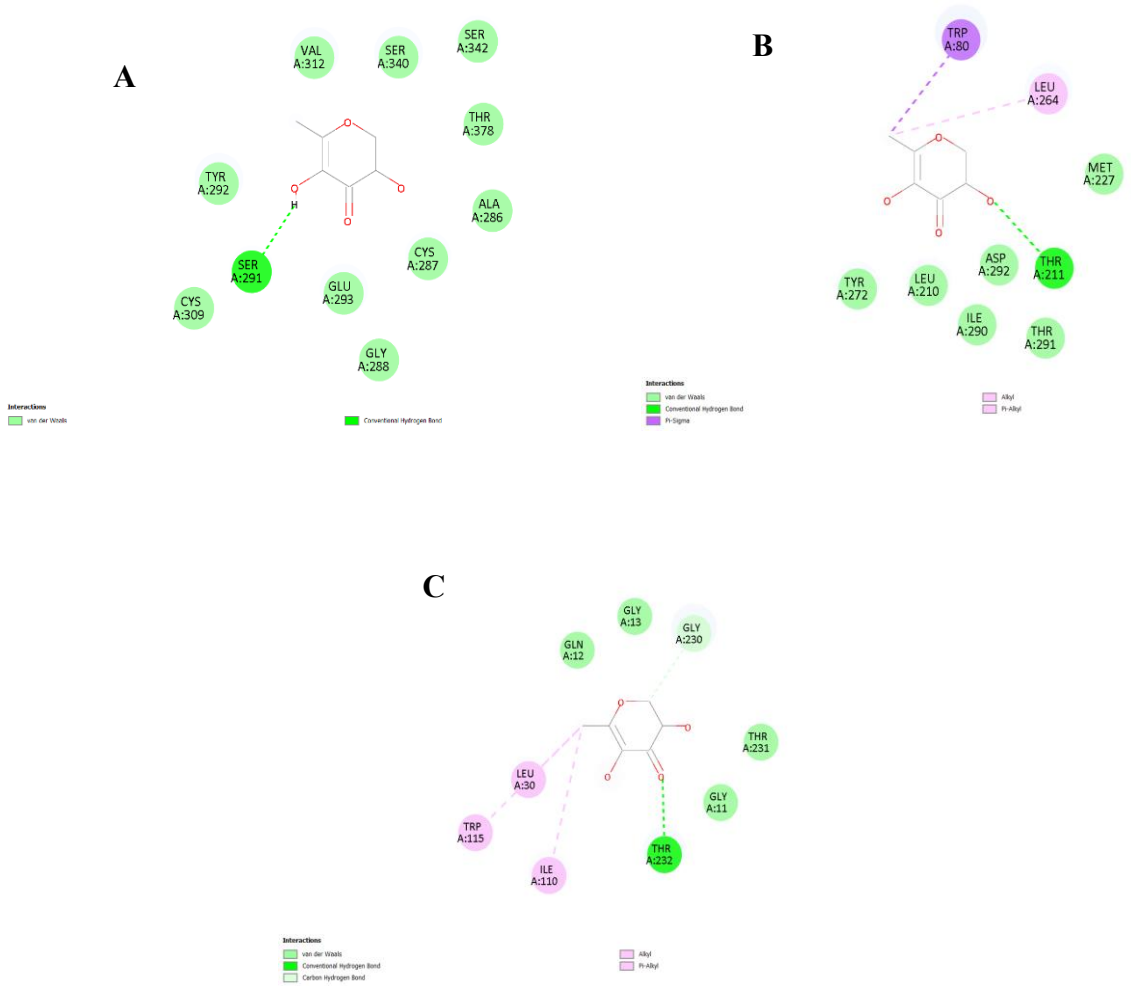

Figure 3: Molecular Docking of receptor and 4H-pyran-4-one, 2,3-dihydro-3,5-dihydroxy-6-methyl-. A) EGFR, B) AKT1, C) BACE-1

Human AKT1

The molecular docking analysis of the selected phytocompounds against AKT Serine/Threonine Kinase 1 demonstrated distinct binding affinities across the nine generated docking conformations. Among all the screened compounds, 4H-pyran-4-one, 2,3-dihydro-3,5-dihydroxy-6-methyl- exhibited the strongest binding affinity with a docking score of −6.5 kcal/mol, indicating a stable interaction within the active binding pocket of AKT1. The docking complex revealed the formation of a conventional hydrogen bond with the THR211 residue, which contributed significantly to ligand stabilization. In addition, van der Waals interactions were observed with amino acid residues including TYR272, LEU210, ILE290, THR291, ASP292, and MET227 (Fig3B). The ligand also demonstrated hydrophobic interactions such as Pi–Sigma interaction with TRP80 and Pi–Alkyl interaction with LEU264, further enhancing the binding stability of the complex. Other selected phytocompounds including 2',4'-Dihydroxypropiophenone, Theobromine, 5-Hydroxymethylfurfural, and 1,2-Benzenediol showed comparatively lower binding affinities ranging from −6.2 to −4.5 kcal/mol. The presence of hydrogen bonding, hydrophobic interactions, and multiple non-bonded contacts suggests that 4H-pyran-4-one, 2,3-dihydro-3,5-dihydroxy-6-methyl- possesses favorable binding characteristics toward AKT1 and may serve as a potential therapeutic candidate for neurodegenerative disorders.

Human BACE-1

The molecular docking analysis of the selected phytocompounds against Beta-Secretase 1 demonstrated different binding affinities across the nine generated docking conformations. Among all the tested compounds, 4H-pyran-4-one, 2,3-dihydro-3,5-dihydroxy-6-methyl- exhibited the strongest binding affinity with a docking score of −5.1 kcal/mol, indicating a favorable interaction within the active site of BACE-1. The docking complex revealed the formation of a conventional hydrogen bond with the THR232 residue, which contributed significantly to the stabilization of the ligand within the binding pocket. In addition, carbon hydrogen bonding interaction was observed with GLY230, while van der Waals interactions were identified with residues GLN12, GLY13, THR231, and GLY11 (Fig3C). The ligand also exhibited hydrophobic interactions including Alkyl and Pi–Alkyl interactions with LEU30, TRP115, and ILE110, further enhancing the binding stability of the protein–ligand complex. Other phytocompounds such as 2',4'-Dihydroxypropiophenone, Theobromine, 5-Hydroxymethylfurfural, and 1,2-Benzenediol showed comparatively lower binding affinities ranging from −5.0 to −3.8 kcal/mol. The presence of hydrogen bonding, hydrophobic interactions, and multiple non-bonded contacts suggests that 4H-pyran-4-one, 2,3-dihydro-3,5-dihydroxy-6-methyl- may serve as a promising bioactive compound targeting BACE-1-associated neurodegenerative pathways.

Molecular Dynamic Simulation

Human EGFR

Molecular dynamics simulation of the EGFR–ligand complex demonstrated stable structural behavior and favorable interaction dynamics throughout the simulation period. The RMSD (Fig4A) profile showed initial fluctuations followed by stabilization around ~0.5 nm, indicating that the system reached equilibrium without significant structural deviation. Residue flexibility analysis (RMSF (Fig4F)) revealed that most residues exhibited low fluctuations, while higher peaks were limited to loop regions, suggesting that ligand binding did not disrupt the overall protein structure. The gradual decrease in solvent accessible surface area (SASA) (Fig4C) and radius of gyration (Rg) (Fig4D) indicates increased compactness and reduced solvent exposure, reflecting a more stable and tightly packed protein–ligand complex. The potential energy (Fig4E) remained consistently stable with minor fluctuations, confirming the thermodynamic stability of the system. Additionally, the presence of persistent hydrogen bonds (Fig4B), averaging around 2–3 throughout the simulation, further supports stable ligand binding within the active site. Overall, these results indicate that the ligand maintains a stable interaction with EGFR under dynamic conditions, suggesting its potential to modulate receptor activity; however, the moderate level of fluctuation observed in RMSD implies a flexible but stable binding mode rather than highly rigid complex formation.

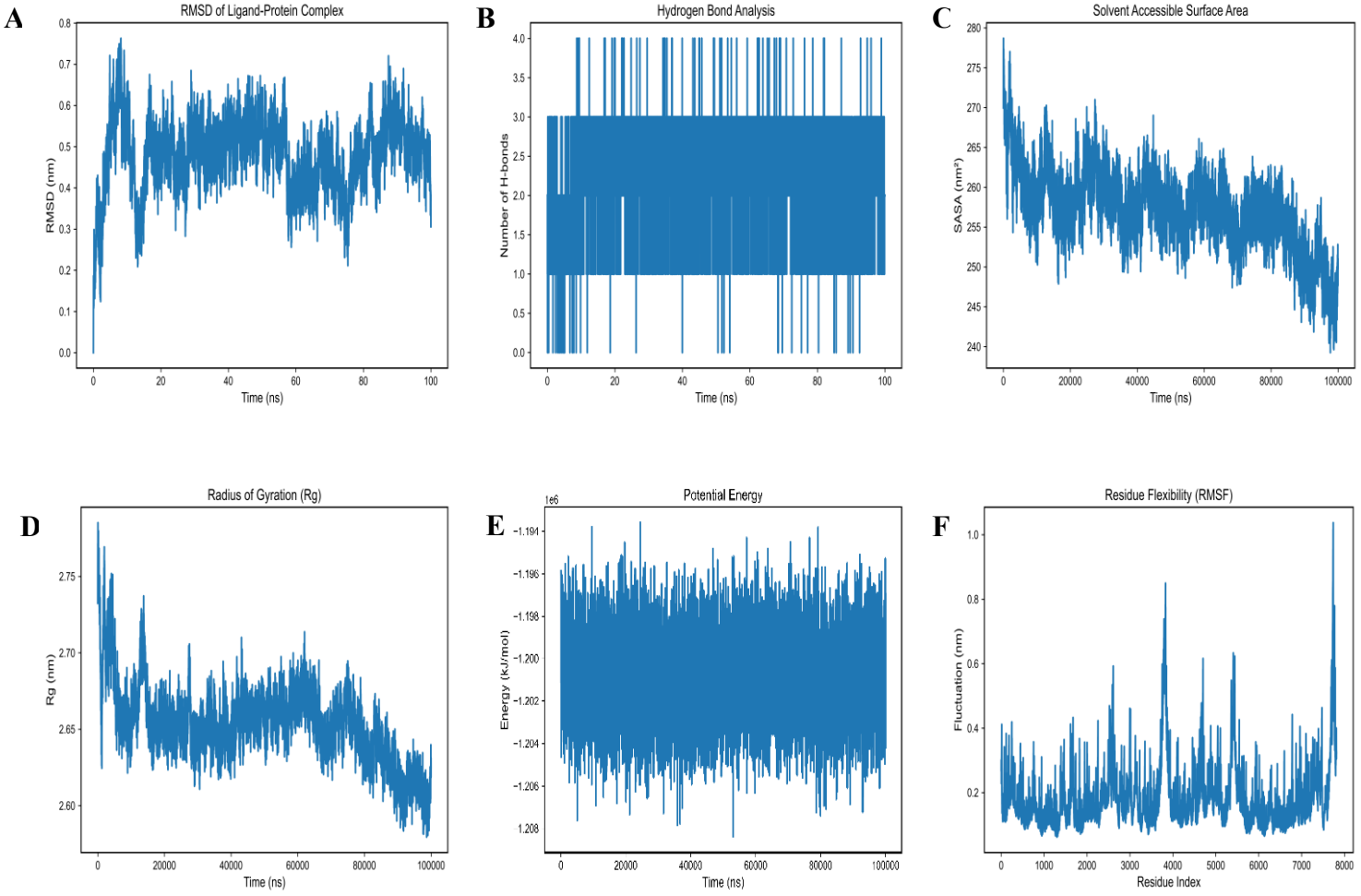

Figure 4: Molecular Dynamic Simulation of EGFR and 4H-pyran-4-one, 2,3-dihydro-3,5-dihydroxy-6-methyl-. A) RMSD, B) Hydrogen Bond, C) SASA, D) Gyration, E) Energy, F) RMSF

Human AKT1

Molecular dynamics simulation of the AKT1–ligand complex demonstrated stable conformational behavior and favorable interaction dynamics throughout the simulation period. The RMSD (Fig5A) profile showed initial fluctuations followed by stabilization around ~0.45–0.65 nm, indicating that the system reached equilibrium without significant structural deviation. The radius of gyration (Rg) (Fig4D) remained relatively stable within the range of ~2.15–2.19 nm, suggesting that the overall compactness of the protein was maintained during ligand binding. Solvent accessible surface area (SASA) (Fig5C) exhibited a gradual decrease over time, reflecting reduced solvent exposure and improved structural packing of the complex. Residue flexibility analysis (RMSF) (Fig5F) revealed that most residues displayed low fluctuations, with higher peaks restricted to loop regions, indicating that ligand binding did not disrupt the structural integrity of the protein core. The potential energy (Fig5E) profile remained consistently stable throughout the simulation, confirming the thermodynamic stability of the system. Additionally, hydrogen bond (Fig5B) analysis showed the formation of 1–3 hydrogen bonds during most of the simulation period, supporting sustained ligand–protein interactions. Overall, these results indicate that the ligand forms a stable and compact complex with AKT1, suggesting its potential to effectively modulate AKT1-mediated signaling pathways involved in neuronal survival and neuroprotection.

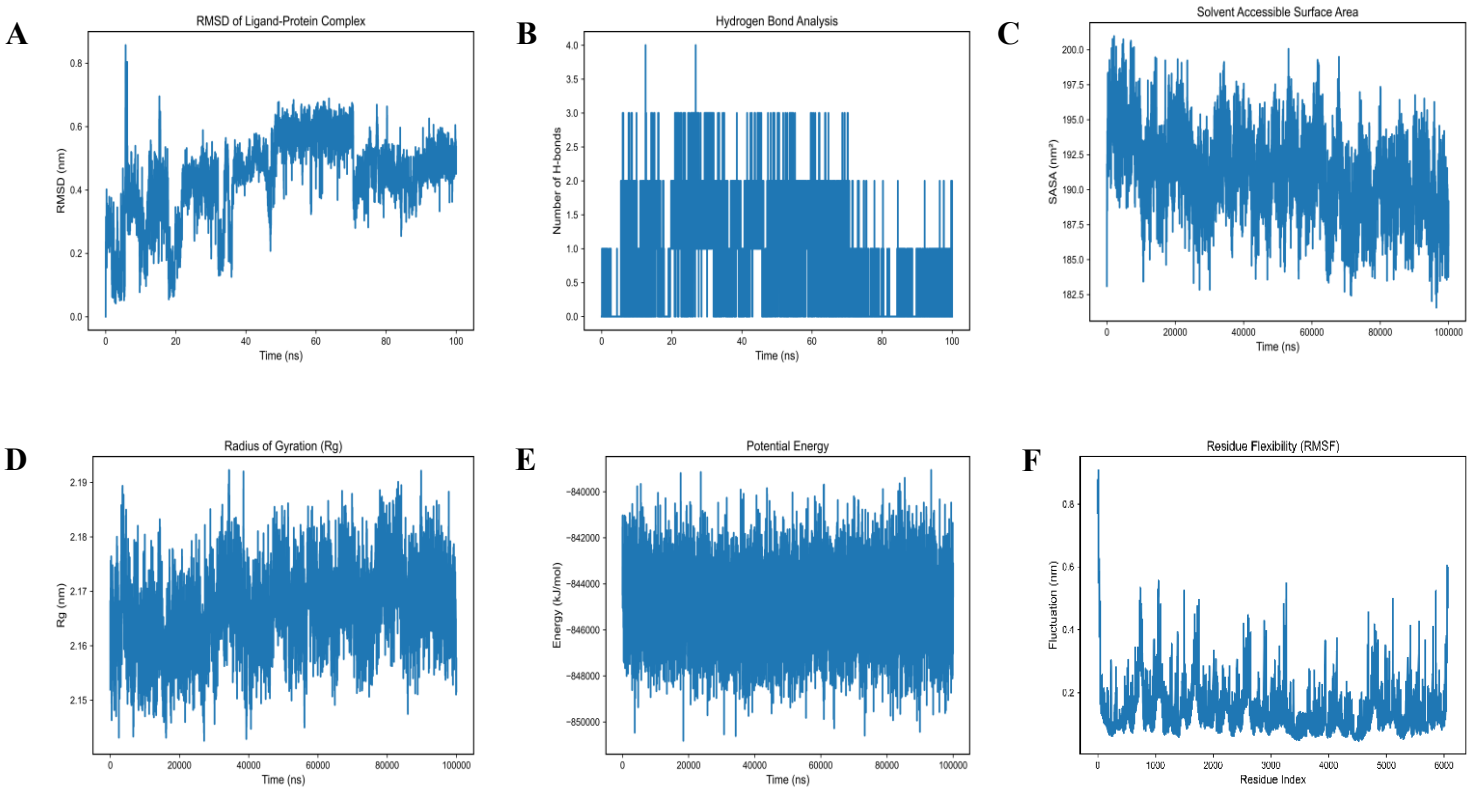

Figure 5: Molecular Dynamic Simulation of AKT1 and 4H-pyran-4-one, 2,3-dihydro-3,5-dihydroxy-6-methyl-. A) RMSD, B) Hydrogen Bond, C) SASA, D) Gyration, E) Energy, F) RMSF

Human BACE-1

Molecular dynamics simulation of the BACE-1–ligand complex demonstrated stable structural and dynamic behavior throughout the simulation period. The RMSD (Fig6A) profile showed moderate fluctuations initially, followed by stabilization within the range of ~0.35–0.50 nm, indicating that the complex reached equilibrium without significant conformational drift. The radius of gyration (Rg) (Fig6D) remained relatively consistent (~2.11–2.17 nm), confirming that the protein maintained its compact structure upon ligand binding. The solvent accessible surface area (SASA) (Fig6C) exhibited a gradual decrease from ~180 to ~160 nm², suggesting reduced solvent exposure and improved packing of the protein–ligand complex. The potential energy (Fig6E) remained stable with minor fluctuations, indicating thermodynamic stability of the system. Hydrogen bond (Fig6B) analysis revealed intermittent formation of 1–4 hydrogen bonds, supporting moderate but sustained interactions between the ligand and BACE-1. Additionally, RMSF (Fig6F) analysis showed limited residue-level fluctuations, with higher flexibility primarily observed in loop regions, while the core residues remained stable. Overall, these findings indicate that the ligand forms a stable and compact complex with BACE-1, supporting its potential role in modulating amyloidogenic pathways relevant to neurodegenerative diseases.

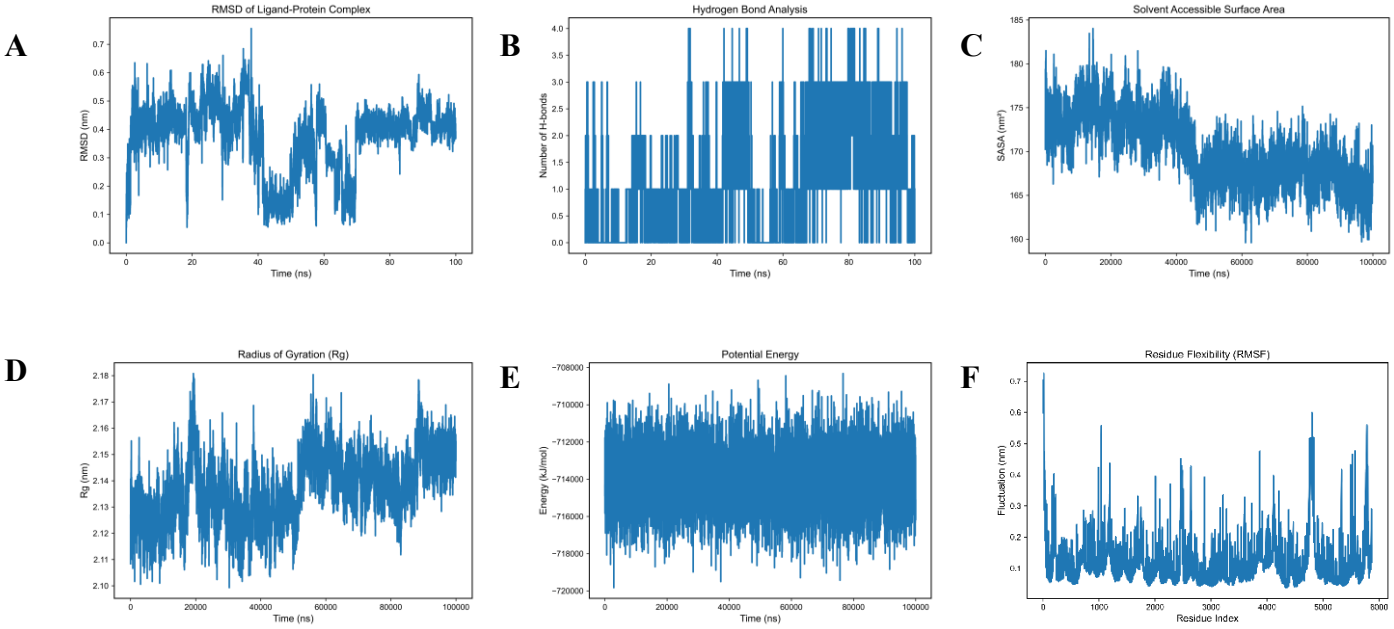

Figure 6: Molecular Dynamic Simulation of BACE-1 and 4H-pyran-4-one, 2,3-dihydro-3,5-dihydroxy-6-methyl-. A) RMSD, B) Hydrogen Bond, C) SASA, D) Gyration, E) Energy, F) RMSF

DISCUSSION

Neurodegenerative disorders are multifactorial diseases characterized by progressive neuronal loss, oxidative stress, neuroinflammation, mitochondrial dysfunction, amyloid aggregation, and impaired cellular signaling pathways. In the present study, an integrated GC–MS-guided network pharmacology, molecular docking, and molecular dynamics simulation approach was employed to elucidate the neuroprotective potential of phytoconstituents identified from the ethanolic root extract of Glycyrrhiza glabra. The obtained findings collectively suggest that the selected phytocompounds, particularly 4H-pyran-4-one, 2,3-dihydro-3,5-dihydroxy-6-methyl- (DDMP), may exert therapeutic effects through multitarget modulation of apoptosis, neuroinflammation, oxidative stress, and amyloidogenic pathways implicated in neurodegeneration.

GC–MS profiling identified 43 volatile and semi-volatile constituents, among which five compounds were prioritized based on structural diversity and reported neuropharmacological relevance. Phenolic and heterocyclic compounds such as DDMP, catechol, and HMF are well known for their antioxidant and radical scavenging activities, which are crucial in preventing reactive oxygen species (ROS)-mediated neuronal damage (Chen et al., 2021). Oxidative stress plays a central role in neuronal degeneration through lipid peroxidation, mitochondrial dysfunction, DNA damage, and activation of apoptotic cascades (Liu et al., 2025). The presence of hydroxyl-rich compounds in the extract therefore provides mechanistic support for the observed interactions with neurodegeneration-associated targets. Similarly, theobromine has been reported to exhibit neuromodulatory and anti-inflammatory effects through adenosine receptor antagonism and regulation of neuronal signaling pathways (Valada et al., 2022).

The network pharmacology analysis further revealed that the identified targets are strongly associated with pathways governing apoptosis, neuroinflammation, amyloid-beta response, and synaptic dysfunction. Hub genes including BACE-1, AKT1, EGFR, TNF, IL-6, TP53, and BCL2 demonstrated high topological significance within the protein–protein interaction network, indicating coordinated regulation of neuronal survival and inflammatory signaling. Chronic neuroinflammation mediated by IL-6 and TNF is recognized as a major contributor to neuronal degeneration through activation of microglial cells and cytokine-mediated oxidative damage (Li et al., 2025). The enrichment of apoptosis-associated pathways and cysteine-type endopeptidase activity further suggests activation of caspase-mediated neuronal death mechanisms, which are hallmark features of Alzheimer's and Parkinson's diseases (Guo et al., 2020). The identified enrichment of amyloid-beta response and Alzheimer disease pathways strongly validates the disease relevance of the selected targets and supports the therapeutic significance of BACE-1 inhibition.

Among the selected targets, AKT1, EGFR, and BACE-1 were prioritized because they collectively represent key signaling nodes involved in neuronal survival, receptor-mediated signaling, and amyloidogenesis. AKT1 is a major regulator of neuronal survival and synaptic plasticity through PI3K/AKT signaling, and reduced AKT activity has been associated with neuronal apoptosis and cognitive impairment in neurodegenerative disorders (Razani et al., 2021). EGFR signaling is involved in neuronal differentiation and inflammatory regulation, although aberrant EGFR activation has been linked with neuroinflammatory progression and glial dysfunction (Jayaswamy et al., 2023). BACE-1 is a critical enzyme responsible for amyloid precursor protein cleavage and amyloid-beta generation, making it one of the most extensively investigated therapeutic targets in Alzheimer's disease (Evin & Hince, 2013).

Molecular docking analysis demonstrated that DDMP consistently exhibited the strongest binding affinity among all screened phytocompounds against EGFR, AKT1, and BACE-1, indicating its multitarget therapeutic potential. The strongest interaction was observed with AKT1 (−6.5 kcal/mol), followed by EGFR (−5.4 kcal/mol) and BACE-1 (−5.1 kcal/mol). The comparatively higher affinity toward AKT1 suggests that DDMP may preferentially modulate neuronal

survival signaling pathways. Importantly, the formation of conventional hydrogen bonds with SER291 in EGFR, THR211 in AKT1, and THR232 in BACE-1 indicates stable ligand anchoring within the active sites of the proteins. Hydrogen bonding is considered a critical determinant of docking stability because it contributes significantly to ligand specificity and binding orientation (Abasi Joozdani et al., 2025). In addition to hydrogen bonding, multiple van der Waals, Pi–Sigma, Pi–Alkyl, and hydrophobic interactions further stabilized the complexes, indicating favorable binding conformations. Similar observations have been reported for phenolic and pyranone-derived compounds exhibiting neuroprotective activity through stable interactions with kinase and amyloidogenic targets (Seba Merin Vinod et al., 2023).

Comparatively, the other phytocompounds including HMF, catechol, theobromine, and 2′,4′-dihydroxypropiophenone exhibited weaker binding affinities across all three targets. Although these compounds possess antioxidant and anti-inflammatory activities, their lower docking scores suggest reduced interaction stability within the active sites relative to DDMP. The superior docking performance of DDMP may be attributed to its hydroxyl-rich pyranone scaffold, which facilitates efficient hydrogen bonding and electrostatic interactions with amino acid residues present in the catalytic pockets of the target proteins. Structurally similar pyranone derivatives have previously demonstrated inhibitory effects against amyloid aggregation and oxidative neuronal damage (Čechovská et al., 2011).

The molecular dynamics simulation studies further validated the docking findings by demonstrating long-term stability of the DDMP–protein complexes under dynamic physiological conditions. The RMSD profiles of EGFR, AKT1, and BACE-1 complexes remained within acceptable fluctuation ranges throughout the 100 ns simulation period, confirming structural equilibration and absence of major conformational instability. Among the three targets, the BACE-1 complex showed the lowest RMSD fluctuation range (~0.35–0.50 nm), suggesting relatively higher structural stability, whereas EGFR displayed slightly greater flexibility, indicative of adaptive ligand accommodation within the binding pocket. Moderate RMSD fluctuations are considered acceptable for stable protein–ligand systems and often reflect conformational adaptability rather than instability (Kumar et al., 2023).

The Rg and SASA analyses further demonstrated progressive structural compactness and reduced solvent exposure following ligand binding, indicating tighter packing of the complexes. Reduced SASA values generally correlate with improved structural stability and decreased solvent accessibility of hydrophobic core residues (Sajal et al., 2026). Persistent hydrogen bonding observed throughout the simulation period further supports sustained ligand interaction with the active sites. The AKT1 complex maintained 1–3 hydrogen bonds consistently, whereas the EGFR and BACE-1 complexes demonstrated intermittent yet stable hydrogen bonding patterns. RMSF analysis showed that fluctuations were primarily localized to loop regions rather than catalytic core residues, indicating that ligand binding did not disrupt the structural integrity of the proteins. Stable potential energy profiles across all simulations additionally confirmed thermodynamic stability of the systems. Collectively, these findings indicate that DDMP forms energetically favorable and conformationally stable complexes with EGFR, AKT1, and BACE-1 under dynamic conditions.

Mechanistically, the multitarget interaction profile of DDMP suggests that it may exert neuroprotective activity through simultaneous suppression of amyloidogenic processing, attenuation of neuroinflammation, and enhancement of neuronal survival signaling. Inhibition of BACE-1 may reduce amyloid-beta production, while modulation of AKT1 signaling could promote neuronal survival and inhibit apoptosis. Concurrent interaction with EGFR may further regulate inflammatory signaling and cellular stress responses. This multitarget mode of action is particularly important in neurodegenerative disorders because single-target therapies often fail to address the complex and interconnected pathology of neuronal degeneration (Lee et al., 2025). Therefore, the observed combined effects on apoptosis, oxidative stress, inflammatory pathways, and amyloid-associated signaling strongly support the therapeutic relevance of DDMP as a potential neuroprotective candidate.

CONCLUSION

The present study demonstrated the neuroprotective potential of phytoconstituents identified from the ethanolic root extract of Glycyrrhiza glabra through an integrated GC–MS, network pharmacology, molecular docking, and molecular dynamics simulation approach. GC–MS analysis identified several biologically active compounds, among which 4H-pyran-4-one, 2,3-dihydro-3,5-dihydroxy-6-methyl- emerged as the most promising multitarget candidate. Network pharmacology and enrichment analyses revealed that the identified targets are strongly associated with neuroinflammation, apoptosis, oxidative stress, amyloid-beta response, and neuronal signaling pathways implicated in neurodegenerative disorders. Molecular docking studies demonstrated favorable binding interactions of the selected compound with key neurodegenerative targets including EGFR, AKT1, and BACE-1, supported by stable hydrogen bonding and hydrophobic interactions. Furthermore, molecular dynamics simulations confirmed the structural and thermodynamic stability of the protein–ligand complexes under dynamic conditions. Collectively, these findings suggest that 4H-pyran-4-one, 2,3-dihydro-3,5-dihydroxy-6-methyl- may serve as a potential multitarget neuroprotective agent capable of modulating amyloidogenic, inflammatory, and apoptotic pathways involved in neurodegeneration. However, further in vitro and in vivo investigations are necessary to validate its therapeutic efficacy and underlying molecular mechanisms.

REFERENCE

1. Abasi Joozdani, F., Amiran, M. R., & Taghdir, M. (2025). Investigation of Akt1 behavior on gold surface from molecular dynamics insight. *Scientific Reports*, *15*(1). https://doi.org/10.1038/s41598-025-20366-2

2. Alzheimer's Association. (2023). 2023 Alzheimer's Disease Facts and Figures. *Alzheimer's & Dementia*, *19*(4), 1598–1695. https://doi.org/10.1002/alz.13016

3. Archana, V. P., Armaković, S. J., Stevan Armaković, Celik, I., J.B. Bhagyasree, Babu, K. V. D., Mithun Rudrapal, Divya, I. S., & Pillai, R. R. (2023). Exploring the structural, photophysical and optoelectronic properties of a diaryl heptanoid curcumin derivative and identification as a SARS-CoV-2 inhibitor. *Journal of Molecular Structure*, *1281*,

135110–135110. https://doi.org/10.1016/j.molstruc.2023.135110
4. Azwanida, N. (2015). A Review on the Extraction Methods Use in Medicinal Plants, Principle, Strength and Limitation. *Medicinal & Aromatic Plants*, *04*(03). https://doi.org/10.4172/2167-0412.1000196
5. Bak, M.-J., Ok, S., Jun, M., & Jeong, W.-S. (2012). 6-Shogaol-Rich Extract from Ginger Up-Regulates the Antioxidant Defense Systems in Cells and Mice. *Molecules*, *17*(7), 8037–8055. https://doi.org/10.3390/molecules17078037
6. Balunas, M. J., & Kinghorn, A. D. (2005). Drug discovery from medicinal plants. *Life Sciences*, *78*(5), 431–441. https://doi.org/10.1016/j.lfs.2005.09.012
7. Čechovská, L., Cejpek, K., Konečný, M., & Velíšek, J. (2011). On the role of 2,3-dihydro-3,5-dihydroxy-6-methyl-(4H)-pyran-4-one in antioxidant capacity of prunes. *European Food Research and Technology*, *233*(3), 367–376. https://doi.org/10.1007/s00217-011-1527-4
8. Chen, Z., Liu, Q., Zhao, Z., Bai, B., Sun, Z., Cai, L., Fu, Y., Ma, Y., Wang, Q., & Xi, G. (2021). Effect of hydroxyl on antioxidant properties of 2,3-dihydro-3,5-dihydroxy-6-methyl-4H-pyran-4-one to scavenge free radicals. *RSC Advances*, *11*(55), 34456–34461. https://doi.org/10.1039/D1RA06317K
9. Essa, M. M., Vijayan, R. K., Castellano-Gonzalez, G., Memon, M. A., Braidy, N., & Guillemin, G. J. (2012). Neuroprotective Effect of Natural Products Against Alzheimer's Disease. *Neurochemical Research*, *37*(9), 1829–1842. https://doi.org/10.1007/s11064-012-0799-9
10. Evin, G., & Hince, C. (2013). BACE1 as a Therapeutic Target in Alzheimer's Disease: Rationale and Current Status. *Drugs & Aging*, *30*(10), 755–764. https://doi.org/10.1007/s40266-013-0099-3
11. Fiore, C., Eisenhut, M., Krausse, R., Ragazzi, E., Pellati, D., Armanini, D., & Bielenberg, J. (2008). Antiviral effects ofGlycyrrhiza species. *Phytotherapy Research*, *22*(2), 141–148. https://doi.org/10.1002/ptr.2295
12. Guo, T., Zhang, D., Zeng, Y., Huang, T. Y., Xu, H., & Zhao, Y. (2020). Molecular and cellular mechanisms underlying the pathogenesis of Alzheimer's disease. *Molecular Neurodegeneration*, *15*(1). https://doi.org/10.1186/s13024-020-00391-7
13. Hardy, J., & Selkoe, D. J. (2002). The amyloid hypothesis of Alzheimer's disease: progress and problems on the road to therapeutics. *Science (New York, N.Y.)*, *297*(5580), 353–356. https://doi.org/10.1126/science.1072994
14. Heneka, M. T., Carson, M. J., El Khoury, J., Landreth, G. E., Brosseron, F., Feinstein, D. L., Jacobs, A. H., Wyss-Coray, T., Vitorica, J., Ransohoff, R. M., Herrup, K., Frautschy, S. A., Finsen, B., Brown, G. C., Verkhratsky, A., Yamanaka, K., Koistinaho, J., Latz, E., Halle, A., & Petzold, G. C. (2015). Neuroinflammation in Alzheimer's disease. *The Lancet. Neurology*, *14*(4), 388–405. https://pmc.ncbi.nlm.nih.gov/articles/PMC5909703/
15. Hopkins, A. L. (2008). Network pharmacology: the next paradigm in drug discovery. *Nature Chemical Biology*, *4*(11), 682–690. https://doi.org/10.1038/nchembio.118
16. Jayaswamy, P. K., Vijaykrishnaraj, M., Patil, P., Alexander, L. M., Kellarai, A., & Shetty, P. (2023). Implicative role of epidermal growth factor receptor and its associated signaling partners in the pathogenesis of Alzheimer's disease. *Ageing Research Reviews*, *83*, 101791. https://doi.org/10.1016/j.arr.2022.101791
17. Karplus, M., & McCammon, J. A. (2002). Molecular dynamics simulations of biomolecules. *Nature Structural Biology*, *9*(9), 646–652. https://doi.org/10.1038/nsb0902-646
18. Kibble, M., Saarinen, N., Tang, J., Wennerberg, K., Mäkelä, S., & Aittokallio, T. (2015). Network pharmacology applications to map the unexplored target space and therapeutic potential of natural products. *Natural Product Reports*, *32*(8), 1249–1266. https://doi.org/10.1039/c5np00005j
19. Kumar, H. B., Suman Manandhar, Rathi, E., Shama Prasada Kabekkodu, Mehta, C. H., Nayak, U. Y., Kini, S. G., & Pai, R. (2023). Identification of potential Akt activators: a ligand and structure-based computational approach. *Molecular Diversity*, *28*(3), 1485–1503. https://doi.org/10.1007/s11030-023-10671-1
20. Kura, A. M., Karukuvelraja Karukuvelraja R, & Pillai, T. G. (2024). Novel Drug Development for Anti-Cholesterol Activity by in silico Analysis: Identification Cholesterol Inhibiting Compounds. *Asian Journal of Biological and Life Sciences*, *13*(1), 48–60. https://doi.org/10.5530/ajbls.2024.13.7
21. Lee, Y., Han, S., Lee, J., Cho, Y., Kim, J.-S., Jeon, Y., Cho, H., Yoo, H., Byun, Y., Kim, T. K., Hong, J.-M., Kim, H., Park, S. Y., Yim, J. H., Kim, S. H., & Jo, D.-G. (2025). A novel multi-target compound mitigates amyloid plaques, synaptic deficits, and neuroinflammation in Alzheimer's disease models. *Archives of Pharmacal Research*, *48*(7-8), 745–764. https://doi.org/10.1007/s12272-025-01562-0
22. LI, S., & ZHANG, B. (2014). Traditional Chinese medicine network pharmacology: theory, methodology and application. *Chinese Journal of Natural Medicines*, *11*(2), 110–120. https://doi.org/10.3724/sp.j.1009.2013.00110
23. Li, X.-Y., Shen, L., & Ji, H.-F. (2025). Exploring the anti-Alzheimer's disease mechanisms of edible medicinal plant Polygonum cuspidatum by integrating network pharmacology and molecular docking. *Industrial Crops and Products*, *231*, 121202. https://doi.org/10.1016/j.indcrop.2025.121202
24. Lindorff-Larsen, K., Piana, S., Palmo, K., Maragakis, P., Klepeis, J. L., Dror, R. O., & Shaw, D. E. (2010). Improved side-chain torsion potentials for the Amber ff99SB protein force field. *Proteins: Structure, Function, and Bioinformatics*, *78*(8), NA-NA. https://doi.org/10.1002/prot.22711
25. Liu, N., Liu, Y., Wang, Y., Feng, C., Piao, M., & Liu, M. (2025). Oxidative cell death in the central nervous system: mechanisms and therapeutic strategies. *Frontiers in Cell and Developmental Biology*, *13*. https://doi.org/10.3389/fcell.2025.1562344
26. Newman, D. J., & Cragg, G. M. (2020). Natural products as sources of new drugs over the nearly four decades from 01/1981 to 09/2019. *Journal of Natural Products*, *83*(3). https://doi.org/10.1021/acs.jnatprod.9b01285
27. Razani, E., Pourbagheri-Sigaroodi, A., Safaroghli-Azar, A., Zoghi, A., Shanaki-Bavarsad, M., & Bashash, D. (2021). The PI3K/Akt signaling axis in Alzheimer's disease: a valuable target to stimulate or suppress? *Cell Stress & Chaperones*, *26*(6), 871–887. https://doi.org/10.1007/s12192-021-01231-3

28. Sajal, H., Mohan, A., Ravi, V., Anjali, K., Raju, R., Rehman, N., & Nadh, A. G. (2026). Computational identification of multi-target natural compounds from Sesbania grandiflora as potential therapeutic agents against Klebsiella pneumoniae. *Scientific Reports*, *16*(1). https://doi.org/10.1038/s41598-026-37613-9
29. Seba Merin Vinod, Sangeetha Murugan Sreedevi, Krishnan, A., Ravichandran, K., Karthikeyan, P., Bharath Kotteswaran, & Rajendran, K. (2023). Complexity of the Role of Various Site-Specific and Selective Sudlow Binding Site Drugs in the Energetics and Stability of the Acridinedione Dye–Bovine Serum Albumin Complex: A Molecular Docking Approach. *ACS Omega*, *8*(6), 5634–5654. https://doi.org/10.1021/acsomega.2c07111
30. Selkoe, D. J., & Hardy, J. (2016). The amyloid hypothesis of Alzheimer's disease at 25 years. *EMBO Molecular Medicine*, *8*(6), 595–608. https://doi.org/10.15252/emmm.201606210
31. Selvaraj, S. P., Lin, K.-H., Lin, W.-C., You, M.-F., Li, T.-L., & Chen, J.-Y. (2024). Rejuvenation of Meropenem by Conjugation with Tilapia Piscidin-4 Peptide Targeting NDM-1 *Escherichia coli*. *ACS Omega*, *9*(27), 29756–29764. https://doi.org/10.1021/acsomega.4c03352
32. Simmler, C., Pauli, G. F., & Chen, S.-N. (2013). Phytochemistry and biological properties of glabridin. *Fitoterapia*, *90*, 160–184. https://doi.org/10.1016/j.fitote.2013.07.003
33. Sinha, S. K., Prasad, S. K., Islam, M. A., Gurav, S. S., Patil, R. B., AlFaris, N. A., Aldayel, T. S., AlKehayez, N. M., Wabaidur, S. M., & Shakya, A. (2020). Identification of bioactive compounds from Glycyrrhiza glabra as possible inhibitor of SARS-CoV-2 spike glycoprotein and non-structural protein-15: a pharmacoinformatics study. *Journal of Biomolecular Structure and Dynamics*, 1–15. https://doi.org/10.1080/07391102.2020.1779132
34. Soundararajan, S., Raja, R. K., S. Vishnu Chitthan, Prasad, S. S., & N. Thajuddin. (2021). Development of wound dressing film using methanolic extracts of freshwater microalgae and determining its wound healing ability. *Current Botany*, 166–173. https://doi.org/10.25081/cb.2021.v12.6986
35. Takemoto-Kimura, S., Suzuki, K., Horigane, S., Kamijo, S., Inoue, M., Sakamoto, M., Fujii, H., & Bito, H. (2017). Calmodulin kinases: essential regulators in health and disease. *Journal of Neurochemistry*, *141*(6), 808–818. https://doi.org/10.1111/jnc.14020
36. Valada, P., Alçada-Morais, S., Cunha, R. A., & Lopes, J. P. (2022). Thebromine Targets Adenosine Receptors to Control Hippocampal Neuronal Function and Damage. *International Journal of Molecular Sciences*, *23*(18), 10510. https://doi.org/10.3390/ijms231810510
37. Wang, L., Yang, R., Yuan, B., Liu, Y., & Liu, C. (2015). The antiviral and antimicrobial activities of licorice, a widely-used Chinese herb. *Acta Pharmaceutica Sinica B*, *5*(4), 310–315. https://doi.org/10.1016/j.apsb.2015.05.005
38. Wang, Y., Nakajima, T., Gonzalez, F. J., & Tanaka, N. (2020). PPARs as Metabolic Regulators in the Liver: Lessons from Liver-Specific PPAR-Null Mice. *International Journal of Molecular Sciences*, *21*(6), 2061. https://doi.org/10.3390/ijms21062061
39. World Health Organization. (2025, March 31). *Dementia*. World Health Organization. https://www.who.int/news-room/fact-sheets/detail/dementia